Estimating Plant Traits of Alpine Grasslands on the Qinghai-Tibetan Plateau Using Remote Sensing

Chengxiu Li, Hendrik Wulf, Bernhard Schmid, Jin-Sheng He, and Michael E. Schaepman, *Senior Member, IEEE*

***Abstract*—Mapping plants traits on the Qinghai-Tibetan Plateau grassland is important for understanding ecosystem functions and how plants respond to global change. Detailed trait maps for the complete Qinghai-Tibetan Plateau are missing. Here, we addressed this issue by combining Sentinel-2 and Landsat-8 multispectral satellite data with field measurements to map and compare plant traits of meadow and steppe communities across the complete Qinghai-Tibetan Plateau. We measured *in-situ* plant-level traits of CHLorophyll content (CHL), specific plant area (SPA = plant area / plant dry mass), and plant dry matter content (PDMC = plant dry mass / fresh mass). We hypothesized that plant-level traits of SPA and PDMC are close to community-weighted means (CWMs) of specific leaf area (SLA) and leaf dry matter content (LDMC) because leaves represent the largest fraction of aboveground biomass in the Qinghai-Tibetan Plateau grasslands. Despite vastly different measurement methods, we found that the remotely sensed traits (SPA and PDMC) correlated with literature-derived leaf traits of CWMs of SLA and LDMC. Both remotely sensed and field-measured results showed that alpine meadow plants reveal a wider range and higher averages of CHL and SPA but lower PDMC compared with alpine steppe plants. These trait differences between vegetation types indicate faster growth of alpine meadow and higher resilience to harsh conditions of alpine steppe, representing differences in adaptation strategies to environmental conditions. Our study demonstrates that remote sensing can be used to estimate plant traits in alpine grasslands with potential applications to retrieve functional diversity and correlated ecosystem functions in future studies.**

***Index Terms*—Chlorophyll content (CHL), Landsat-8, Leaf Dry Matter Content (LDMC), Plant Dry Matter Content (PDMC), Qinghai-Tibetan Plateau, Sentinel-2, Specific Leaf Area (SLA), Specific Plant Area (SPA), vegetation indices.**

I. Introduction

PLANT traits are physiological and morphological features of an organism [1]. Plant traits such as leaf nitrogen concentration, specific leaf area (SLA), and leaf dry matter content (LDMC) are related to plant physiological processes such as light capture and photosynthetic rate and can hence provide indications of functional strategies of plants in different environmental conditions [2], [3]. These correlations make these traits key to predict ecosystem functions, such as primary productivity [4]. Within the recently emerging discussion on essential biodiversity variables derived by remote-sensing techniques [5], these traits have been listed as key plant functional traits [6]. Their relevance for plant and ecosystem functioning is reflected by their incorporation into dynamic global vegetation models to simulate ecosystem functions such as vegetation carbon dynamics and hydrological processes [7], [8]. Therefore the retrieval of these plant traits is important, in particular for grasslands, which cover more than 40% of the terrestrial land surface and are responsible for important ecosystem services such as carbon sequestration and forage production [4].

In alpine grasslands, leaf-level trait measurements are close to plant-level trait measurements, because herbaceous plants do not have prominent aboveground stems and in addition stems are green and thus are physiologically similar to leaves. This is especially the case for the grassland on the Qinghai-Tibetan Plateau, where aboveground vegetation is dominated by graminoids and rosette- and cushion-forming plants [9], [10]. For these types of vegetation, aboveground part of plants can therefore be considered as equivalent to "big-leaf structures" when measuring traits [11]. Regarding photosynthesis and primary productivity it is hence appropriate to work with aboveground plant-level traits rather than leaf-level traits in these vegetation types. Plant-level traits aggregated to the community level allow for an easier integration with spaceborne remote-sensing datasets, which typically collect spectral information of grasslands at the canopy level. Therefore, we approximate Specific Plant Area (SPA = plant area/plant dry mass) and Plant Dry Matter Content (PDMC = plant dry mass/plant fresh mass) to Community-Weighted Means (CWMs) of SLA and LDMC. The proxy traits of SPA and PDMC can be estimated for extensive area from remotely sensed spectra.

Manuscript received November 2, 2017; revised March 5, 2018 and April 1, 2018; accepted April 3, 2018. The work of C. Li, B. Schmid, and M. E. Schaepman was supported by the University of Zurich Research Priority Program on "Global Change and Biodiversity" (URPP GCB). *(Corresponding author: Chengxiu Li.)*

C. Li, H. Wulf, B. Schmid, and M. E. Schaepman are with the Remote Sensing Laboratories, Department of Geography, University of Zurich, Zurich CH-8057, Switzerland (e-mail: chengxiu.li@geo.uzh.ch; hendrik.wulf@geo.uzh.ch; bernhard.schmid@uzh.ch; michael.schaepman@geo.uzh.ch).

J.-S. He is with the Department of Ecology, College of Urban and Environmental Sciences, Peking University, Beijing 100871, China (e-mail: jshe@pku.edu.cn).

This paper has supplementary downloadable material available at http://ieeexplore.ieee.org. The Word .doc contains three supporting figures of predicting Canopy CHL, above ground biomass and Plant Dry Matter Content using different vegetation indices. Fig. S1 shows linear regression between vegetation indices and canopy CHL. Fig. S2 shows a linear calibration model of Landsat-8 NDVI to predict aboveground biomass. Fig. S3 shows linear regression between vegetation indices and Plant Dry Matter Content (PDMC). The Excel file includes a table containing species SLA and LDMC value from literature and the converted species SLA and LDMC used in our study. The total file size is 1.78 MB.

Color versions of one or more of the figures in this paper are available online at http://ieeexplore.ieee.org.

Digital Object Identifier 10.1109/JSTARS.2018.2824901

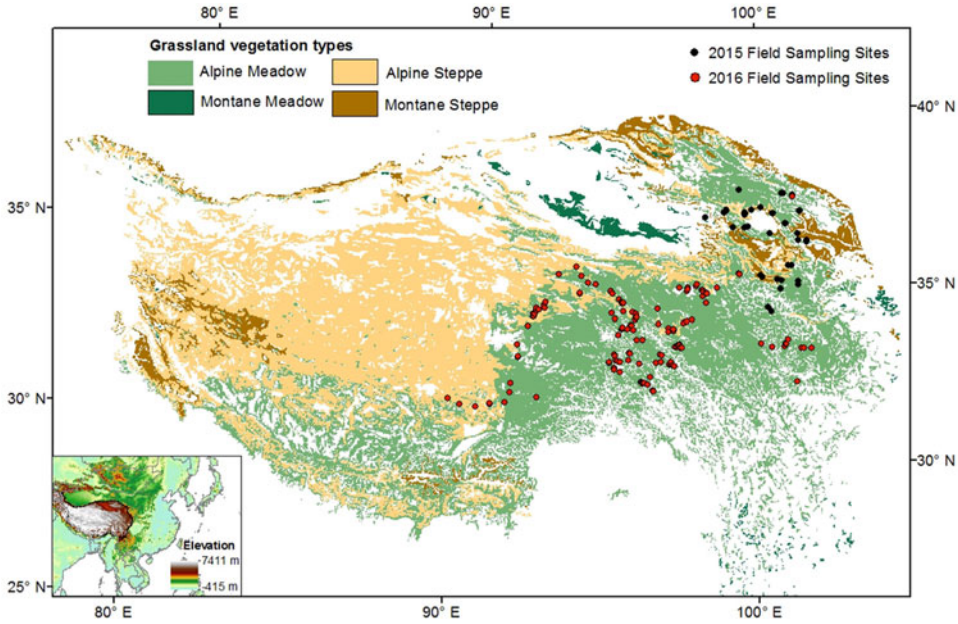

Fig. 1. Distribution of grassland vegetation types [40] on the Chinese part of the Qinghai-Tibetan Plateau and sampling site locations used in this study (2015 = black dots, 2016 = red dots). Inset indicates elevation data of the extended area based on the NASA Shuttle Radar Topographic Mission (SRTM Version 4) [94].

Remotely sensed vegetation spectra provide information on plant physiological (e.g., pigment, SLA, and LDMC) and morphological traits (e.g., leaf area) [12], [13]. Physical radiative-transfer models and empirical statistical models have been developed to estimate plant physiological and morphological traits [12]–[17] using remotely sensed data. Employing these models, plant traits such as CHLorophyll content (CHL) [18]–[20], SLA [14], [21]–[24], and LDMC [16], [25], [26] were successfully derived. Although LDMC and SLA are crucial plant traits for understanding plant functioning, studies on estimating CHL, SLA, and LDMC for grassland ecosystems using spectral data are relatively rare [12], [26]–[30]. In an earlier study, a radiative-transfer model was inverted to estimate CHL and leaf mass per area (LMA = 1/SLA) for a grassland ecosystem, but the retrieved plant traits were not validated with the field-measured traits [12]. A further local study applied partial least squares regressions to estimate plant physiological traits at leaf and canopy level using field spectroradiometer data [28]. To our knowledge, no study so far has estimated plant traits of LDMC and SLA for grassland ecosystems using remote-sensing data. Furthermore, we are not aware of studies that attempted to estimate plant traits using remote sensing across the whole Qinghai-Tibetan Plateau. Existing studies from the Qinghai-Tibetan Plateau working with plant traits typically remained at a plot scale and explored the relationships between local plant traits and environmental variables such as soil and climatic variables [31], [32]; grazing level [33]–[35]; and elevation [36].

Estimating plant traits using remote sensing over the complete Qinghai-Tibetan Plateau can help us to characterize the current ecosystem state in terms of plant functioning. Such an assessment cannot be realized on the ground with a realistic financial budget due to the vast extent and limited accessibility of the Qinghai-Tibetan Plateau. Furthermore, remote sensing enables repeated assessments over time, which can help us to identify changes of plant traits. Tracing changes of plant traits on the Qinghai-Tibetan Plateau is particularly important as the area is prone to be affected by the climate change due to its very high altitude and corresponding harsh conditions [37]. This is also mirrored in grassland degradation processes that have been observed in different intensities over the Plateau and have been related to anthropogenic activities (e.g., overgrazing) but also natural process triggered by a changing climate [38]. Besides such monitoring activities, spatially continuous data on plant traits can also help us to better understand the current distribution of plant functional types and plant strategy groups over the Plateau. The latter could be crucial to understand potential threats for certain plant communities under climate change scenarios.

In this study, we use field-measured values of canopy CHL, specific plant area (SPA), and plant dry matter content (PDMC) aggregated to the canopy level to derive remotely sensed proxies of these traits for the entire Qinghai-Tibetan Plateau. Furthermore, we show how remotely sensed traits of SPA and PDMC correspond to literature-derived Community-Weighted Means (CWMs) of SLA and LDMC in alpine grasslands. Finally, based on the plant traits estimated via remote sensing, we investigate plant trait differences between four vegetation types to identify differences in plant adaptation strategies.

II. Data

A. Study Area and Vegetation Types

The Qinghai-Tibetan Plateau covers an area of approximately 2.5×10^6 km^2 with complex terrain and an average elevation of more than 4000 m a.s.l (see Fig. 1). The area shows a decreasing thermal and moisture gradient from southeast to northwest [39], where the mean annual temperature ranges from 15.5 to –5.0 °C and the precipitation ranges from more than 1000 mm/yr to less than 100 mm/yr [9], [39].

TABLE I
SENTINEL-2 VEGETATION INDICES FOR CANOPY CHL ESTIMATION

Vegetation indices	Formula	Reference
CIred-edge	$R_{783}/R_{705} - 1$	[70], [95], [96]
CIgreen	$R_{783}/R_{560} - 1$	[70], [95], [96]
MCARI /OSAVI	$\frac{[(R_{740} - R_{705}) - 0.2(R_{740} - R_{560})](R_{740}/R_{705})}{(1 + 0.16)\,(R_{740} - R_{705})/(R_{740} - R_{705} + 0.16)}$	[2], [97], [98]
TCARI/OSAVI	$\frac{3[(R_{740} - R_{705}) - 0.2(R_{740} - R_{560})(R_{740}/R_{705})]}{(1 + 0.16)\,(R_{740} - R_{705})/(R_{740} - R_{705} + 0.16)}$	[2], [98]

TABLE II
LANDSAT-8 VEGETATION INDICES FOR PDMC AND ABOVEGROUND BIOMASS ESTIMATION

Vegetation indices	Formula	Reference
EVI	$(R_{851} - R_{655})/(R_{851} + 6R_{655} - 7.5R_{482} + 1)$	[99]
SAVI	$(R_{851} - R_{655})/(R_{851} + R_{655} + 0.5) * (1.5)$	[100]
NDVI	$(R_{851} - R_{655})/(R_{851} + R_{655})$	[101]
MSAVI	$(2R_{851} + 1 - \sqrt{(2R_{851} + 1)^2 - 8(R_{851} - R_{655})})/2)$	[102]

R_x refers to the reflectance at wavelength x nm

The most dominant vegetation types are alpine steppe and alpine meadow, which occupy 22.4% and 23% of the total Plateau area, respectively [40]. Both vegetation types are predominantly located at elevations above 4000 m [9], [10], [41]. Alpine meadow occurs in the south-eastern humid highlands [9], [41]. Alpine steppe prevails in the more (semi) arid central and western highlands with low precipitation (<350 mm/yr) [10]. Transitional zones with mixed alpine meadow and alpine steppe occur in the central part of the Qinghai-Tibetan Plateau [42]. Montane steppe and montane meadow are less dominant grassland vegetation types, occupying only 4% and 1% of the whole Plateau area [40]. These vegetation types occur predominantly at altitudes <4000 m. Montane meadow mainly occurs in the northeast Qaidam Basin. Montane steppe is distributed on the northern margin of the Plateau and around the Qaidam Basin [43].

B. Satellite Data

We used the Google Earth Engine [44] to process all available satellite data of Landsat-8 surface reflectance [45], Sentinel-2 Top Of the Atmosphere (TOA) reflectance [46], Moderate Resolution Imaging Spectroradiometer (MODIS) Land Cover Type product (MCD12Q1) [47], and MODIS Leaf Area Index (LAI) product (MCD15A3H) [48]. We refer to MODIS LAI as Plant Area Index (PAI) in our context. We applied the Landsat-8 surface reflectance Quality Assurance band (CFmask) [49], [50] and the MCD15A3H quality control band (FparLai_QC) to mask cloud, snow, and cloud shadow [51], [52]. We used an adjusted Landsat cloud-score algorithm to mask clouds in Sentinel-2 TOA reflectance data [53].

Given the availability of the red-edge bands in Sentinel-2, we used Sentinel-2 data to estimate canopy CHL. In the study area, Sentinel-2 data are available in the Google Earth Engine as Level 1C TOA reflectance data from 2016 onwards. In all, 3560 Sentinel-2 TOA reflectance scenes spanning from July to August 2016 were selected to calculate red-edge band vegetation indices (see Table I) for estimating canopy CHL. Landsat-8 surface reflectance data were available for both years, 2015 and 2016, which enabled us to link Landsat-8 data to all our field measurements. Therefore, we used Landsat-8 surface reflectance data to calculate vegetation indices (see Table II) for predicting dry aboveground biomass and PDMC. In total, 1542 Landsat-8 surface reflectance scenes were selected, which covered the whole study area from June to September in 2015 and 2016. We used the MCD15A3H LAI product with 4-day time-steps and 500 m resolution from June to September in 2015 and 2016 to calculate the SPA, and MODIS Land Cover Type product (MCD12Q1) from 2013 to mask out all land cover types other than grasslands.

C. Data on Vegetation Types

The vegetation-type data were acquired from the Chinese vegetation atlas (scale 1:1 000 000). This atlas is based on the results of nationwide vegetation surveys and complementary data from aerial remote-sensing devices and satellite images, as well as geological, pedological, and climatological data [40]. The atlas provides a complete map of vegetation types and is frequently used in studies on the Qinghai-Tibetan Plateau [39], [54]. This dataset was used to build the link between plant traits and vegetation types to further evaluate how plant traits differed among vegetation types. We provided a general overview of the applied data and methods as flowchart (see Fig. 2).

III. METHODS

A. Field-Measured Plant Traits

Field data were collected on 59 sites over an area extending 1225 km in north-south and 695 km in east-west direction (see Fig. 1). The sampling sites cover three vegetation types (i.e., alpine meadow, alpine steppe, and montane steppe) along an east-west gradient (see Fig. 1). Montane meadow was not considered in the study because of its limited distribution area. The data acquisition date coincided with the peak of the growing season (late July to mid-August) in 2015 and 2016. The montane steppe sampling sites were located at lower altitudes (average 3200 m) compared to the alpine steppe sampling sites (average 4800 m). Alpine meadow sampling sites were distributed along an elevation gradient ranging from 2800 to 5200 m. All sampling sites were selected to have homogeneous vegetation cover. At each site, four quadrats of one square meter were sampled within an area of 250 × 250 m. Each of the four quadrats was representative of the wider surrounding (30 × 30 m) to represent approximately the extent of a Landsat satellite image pixel.

In each quadrat, we conducted field measurements of 1) species cover, 2) SPAD leaf absorbance (SPAD-502Plus Chlorophyll Meter, KONICA MINOLTA, INC., Osaka, Japan) of abundant species, 3) plant area index (PAI), and 4) plot aboveground plant fresh biomass and dry biomass. Species cover was

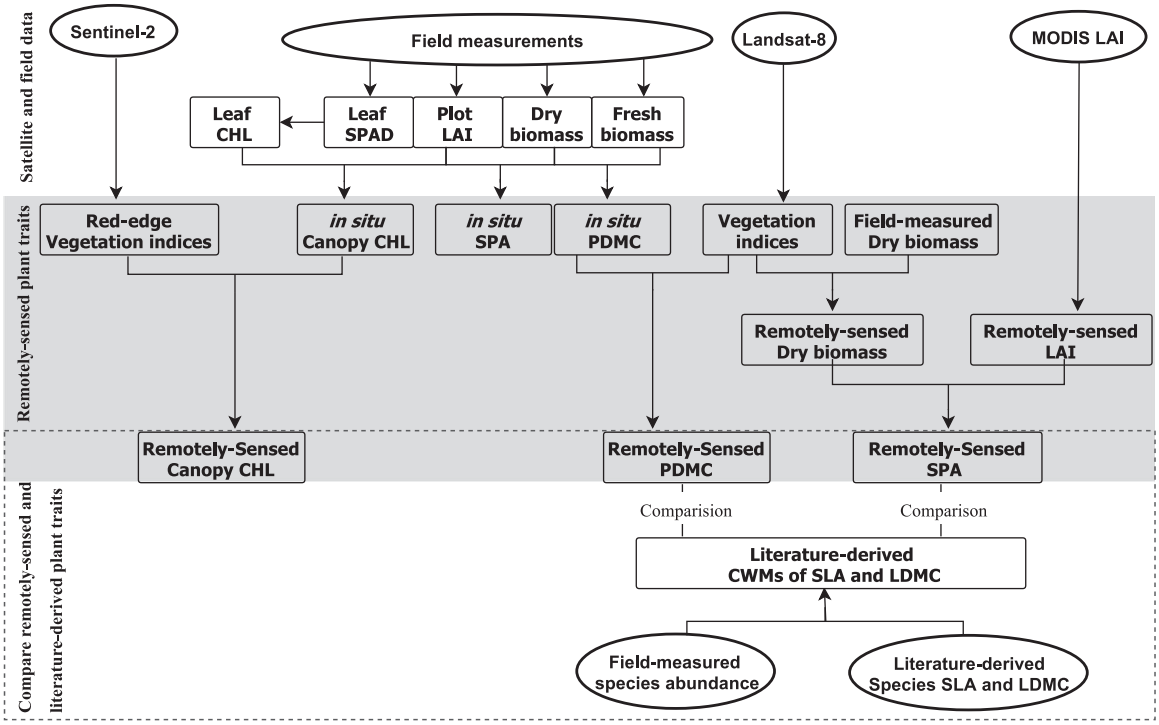

Fig. 2. Flowchart displaying data and methods to derive plant traits.

averaged from 2 to 3 investigator estimations. For each species, 12–15 SPAD recordings were taken from different leaves and averaged as species SPAD value [55], [56]. The CWM of SPAD values was obtained by averaging the coverage-weighted species-level SPAD values for each plot. CWMs of SPAD values were converted to CHL values using the following equation [56]:

$$\text{Leaf CHL } \left(\text{mg/m}^2\right) = \text{SPAD } \times 16.844 - 192.84. \quad (1)$$

This model was calibrated from grass 14 CHL measurements in the laboratory and corresponding SPAD values collected in the field [56]. Finally, CHL values were upscaled to canopy CHL by multiplication with the PAI values [55], [57]–[60]

$$\text{Canopy CHL} = \text{leaf CHL} \times \text{PAI}. \quad (2)$$

We refer PAI to LAI because all aboveground green parts of a plant were measured instead of only leaves. The PAI measurements were based on digital hemispherical photographs (DHPs) and calculated with the CAN-EYE software [61], [62]. In each quadrat, 8–10 downward pointing photos were taken with automatic exposure settings. Aboveground peaking plant fresh biomass was measured by clipping, weighing to an accuracy of ± 0.01 g, and then drying for 48 h at 65 °C to obtain a constant dry aboveground biomass. In total, PAI was measured in 228 plots, and plant fresh and dry aboveground biomass was measured in 172 plots.

To estimate traits in a mixed-species community, leaf traits are typically measured for all species and aggregated to the community mean weighted by species abundances in terms of plant cover or aboveground plant biomass proportions (CWMs) [63]. Ideally, CWMs of traits would be averaged from traits of all plants within a community without requiring taxonomic information of plant species [64]. This way of trait measurements within a community is more efficient and accurate because it is independent of the taxonomic information and measures all plants within a community. Here, we measured traits within a community directly from vegetation harvests, to average plant-level traits of all plants of a community without requiring taxonomic information. Specifically, we derived the ratio of aboveground plant area and plant dry mass within a community and used it as a proxy of the CWMs of SLA. Similarly, we used the ratio of aboveground plant fresh mass and dry mass within a community as a proxy of the CWMs of LDMC. In other words, we refer to the ratio between PAI and aboveground plant dry biomass within a field plot as SPA and to the ratio between aboveground plant fresh biomass and dry biomass as PDMC throughout this study. We hypothesize that in alpine grasslands, SPA and PDMC are close to CWMs of SLA and LDMC because leaves represent a large part of aboveground biomass and aboveground nonleaf structures in this vegetation (e.g., stems or graminoid inflorescences) are also green and photosynthesizing. The SPA and PDMC refer to the measurement at the community level, which match the plant traits estimate from remote sensing at the canopy level.

Literature-derived CWMs of SLA and LDMC were calculated using our field-measured species abundance values (cover proportions of dominant species) and SLA and LDMC values of these species reported in earlier studies conducted on the Qinghai-Tibetan Plateau [65]–[68] (Table S1). In total 121 species were recorded in 198 plots. For 42 species SLA values and 29 species LDMC values were averaged from the same species values in the literature [65]–[68], and 101 species SLA values and 94 species LDMC values were averaged from the same genus values in the literature [65]–[68]. For 19 and 26 species no published SLA and LDMC values, respectively,

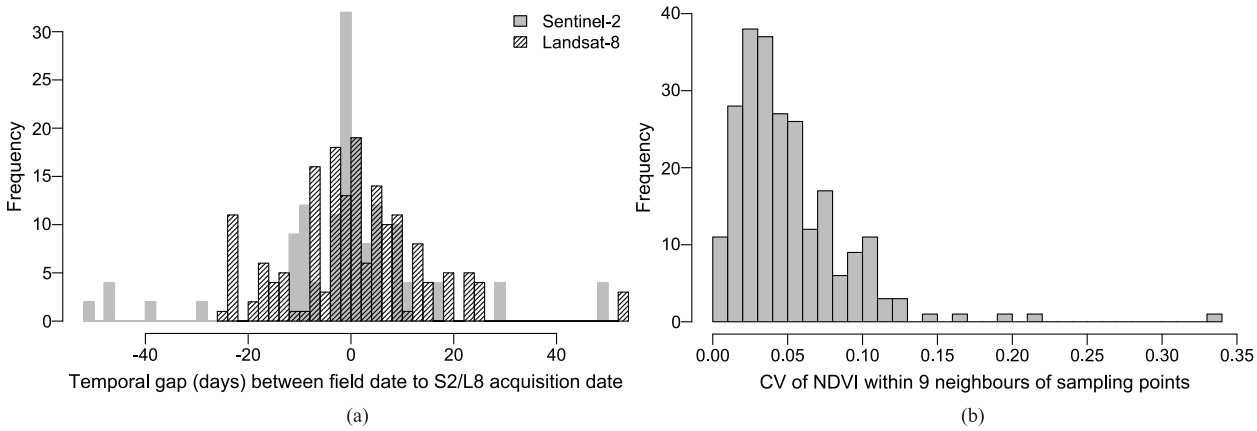

Fig. 3. Linking field and satellite measurements spatially and temporally. (a) Frequency histogram of the Coefficient of Variation (CV) of Sentinel-2 NDVI (10 m) within nine neighboring sample points. (b) Frequency histogram of temporal gaps (days) between field measurement date and Sentinel-2 (S2) MCARI/OSAVI acquisition date.

were available. To represent the community means of the plots, CWMs of SLA and LDMC were calculated for all plots where SLA and LDMC values for more than four species were available. Using this rule, we could derive CWMs of SLA for 18 plots and CWMs of LDMC for 28 plots. In these plots, the species for which SLA and LDMC values were available accounted for more than 38% of plant coverage in all cases. Considering the homogeneity rule that was applied to select the field plots, we hypothesized that these coverages were sufficient to derive a meaningful estimate of the CWMs of the two traits.

B. Remotely Sensed Plant Traits

1) Canopy CHL: The reflectance in the red-edge region is mainly affected by chlorophyll density [18] and remains highly sensitive to a wide range of chlorophyll-content variability [19], [69]. The empirical red-edge indices adapted for Sentinel-2 data have been successfully applied to predict CHL in different ecosystem types [15], [18], [70], [71]. In this study, we used the red-edge bands to predict canopy CHL. These red-edge vegetation indices include the ratio of the Modified Chlorophyll Absorption Ratio Index and the Optimized Soil-Adjusted Vegetation Index (MCARI/OSAVI), the ratio of the Transformed Chlorophyll Absorption Ratio Index and the Optimized Soil-Adjusted Vegetation Index (TCARI/OSAVI), the green chlorophyll index (CIgreen), and the red-edge chlorophyll index (CI red-edge) [19], [72] (see Table I). We compared the performance of these indices and chose the best index to predict canopy CHL throughout the Qinghai-Tibetan Plateau.

2) Specific Plant Area (SPA): SPA was calculated from the ratio between PAI and aboveground plant dry biomass. PAI values were taken from the MODIS product MCD15A3H at 500 m spatial resolution. Aboveground biomass was estimated using an empirical model developed from Landsat-8 vegetation indices (see Table II) and field-measured aboveground biomass. To match the spatial resolution of PAI (500 m) and aboveground biomass (30 m), the aboveground biomass was resampled to 500 m using a bilinear approach. Therefore, SPA was retrieved at a 500 m spatial scale.

3) Plant Dry Matter Content (PDMC): An empirical model was developed from Landsat-8 vegetation indices and field-measured PDMC to estimate PDMC for the whole Qinghai-Tibetan Plateau.

C. Linking Field and Satellite Measurements

We linked remotely sensed vegetation indices and field-measured plant traits temporally and spatially by extracting the closest satellite pixels with respect to the individual field sampling locations and dates. To evaluate how satellite and field measurements match temporally, we calculated temporal gaps (days) between the satellite acquisition dates and field-measured dates. For 90% of the sampling sites, Sentinel-2 and Landsat-8 images were available within 20 days of field measurements. To test the representativeness of field samples $(1 \times 1$ m) for the satellite pixels (30×30 m), we evaluated the homogeneity of the neighborhoods (30×30 m) of sampling locations by calculating the coefficient of variation of NDVI. Taking advantage of the 10-m spatial resolution of Sentinel-2 reflectance in the visible bands, coefficients of variation of NDVI of nine neighbors for each sampling point were calculated (see Fig. 3). Lower coefficients of variation values indicate a higher homogeneity of neighborhoods. The coefficient of NDVI variation within 30-m neighborhoods of sampling points showed that 85% of sampling points were located in homogenous neighborhoods with a coefficient of surrounding NDVI variation less than 0.1 (see Fig. 3).

D. Statistical Modeling and Validation Methods for Remotely Sensed Plant Traits

We applied linear regression models to quantitatively link the field-measured plant traits with Sentinel-2 red-edge vegetation indices and Landsat-8 vegetation indices (see Tables I and II). To evaluate model performance, the data were randomly split into two parts, using three-quarters of the data for model calibration and one-quarter for validation. After 500 model runs, we calculated the mean R^2 and the relative Root-Mean-Square Error (rRMSE (%)) as the ratio between RMSE and the mean of measured plant traits. The models with the highest accuracy

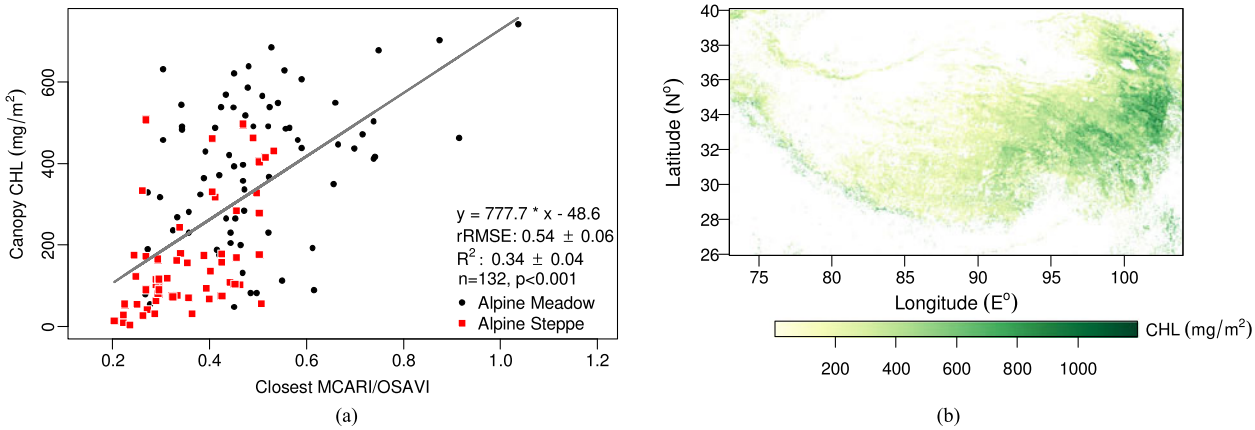

Fig. 4. Remotely sensed canopy CHL on the Qinghai-Tibetan Plateau grasslands. (a) Linear calibration model of MCARI/OSAVI to predict canopy CHL. (b) Canopy CHL with a spatial resolution of 20 m in the 2016 peak-growing season.

(highest R^2 and lowest rRMSE) were applied to the Sentinel-2 red-edge and Landsat-8 vegetation index to generate the canopy CHL, aboveground dry biomass, and PDMC maps for the whole study area.

E. Kernel Density Estimation for Visualization of Plant Traits of Different Vegetation Types

To assess potential plant trait differences between the four examined vegetation types, we applied a kernel density estimation to visualize the distribution of plant traits for the examined vegetation types and visually compare their trait differences [73], [74]. This analysis was conducted for both field-measured and remotely sensed plant traits, namely at a 1-m scale based on field-measured plant traits and vegetation types, and at a 1-km scale based on the remotely sensed plant traits and vegetation types from the Chinese vegetation atlas. We used the 1-km scale to optimize the computation time.

IV. Results

A. Plant Traits

1) Canopy CHL: The red-edge vegetation index MCARI/OSAVI was able to predict 34% of field-measured canopy CHL variation with an rRMSE of 0.54 outscoring the CIgreen ($R^2 = 0.25, \text{rRMSE} = 0.57$), CI red-edge ($R^2 = 0.31, \text{rRMSE} = 0.55$), and the TCARI/OSAVI ($R^2 = 0.05, \text{rRMSE} = 0.65$) indices (Fig. S1). The MCARI/OSAVI underestimated the field-measured canopy CHL at lower MCARI/OSAVI values (MCARI/OSAVI < 0.5) but overestimated the field-measured canopy CHL at higher MCARI/OSAVI values (MCARI/OSAVI > 0.5) (see Fig. 4). Based on the MCARI/OSAVI index, we predicted the canopy CHL in the study area (see Fig. 4). The mean Canopy CHL of the entire Plateau in the 2016 peak growing season was 342 mg/m^2. The CHL map illustrates the decreasing gradient of canopy CHL from the eastern meadow-dominated part to the western steppes-dominant part on the Qinghai-Tibetan Plateau (see Fig. 4).

2) Specific Plant Area (SPA): The regression model developed from Landsat-8 NDVI ($R^2 = 0.55, \text{rRMSE} = 0.23$) (Fig. S2) showed the highest accuracy in predicting field-measured aboveground dry biomass in comparison with the model developed from vegetation indices MSAVI ($R^2 = 0.53, \text{rRMSE} = 0.24$), EVI ($R^2 = 0.54, \text{rRMSE} = 0.23$), and SAVI ($R^2 = 0.53, \text{rRMSE} = 0.24$). The NDVI model was hence used to generate an aboveground biomass map, which was combined with the PAI product to predict SPA. The remotely sensed SPA calculated from a ratio between PAI (MCD15A3H) and aboveground dry biomass (Landsat-8 NDVI) showed moderate consistency with the field-measured SPA (rRMSE = 0.49 and $R^2 = 0.22$) (see Fig. 5). Remotely sensed SPA are also correlated with CWMs of SLA calculated form literature data on the Qinghai-Tibetan Plateau, with R^2 of 0.2 and rRMSE of 0.15 (see Fig. 6). However, remotely sensed SPA values were on average 53 g/cm^2 lower than CWMs of SLA.

3) Plant Dry Matter Content (PDMC): The regression model developed from Landsat-8 EVI (see Fig. 7) ($R^2 = 0.53, \text{rRMSE} = 0.144$) showed the highest accuracy in predicting field-measured PDMC in comparison with the models that used MSAVI ($R^2 = 0.525, \text{rRMSE} = 0.144$), NDVI ($R^2 = 0.522, \text{rRMSE} = 0.144$), and SAVI ($R^2 = 0.526, \text{rRMSE} = 0.145$) vegetation indices (Fig. S3). The predicted PDMC in the 2016 peak growing season showed an opposite spatial pattern compared with predicted canopy CHL and SPA, with lower values in the northeast of the meadow grassland and higher values in sparsely vegetated alpine steppe area in the West (see Fig. 7). We found that remotely sensed PDMC correlated with the literature-derived CWMs of LDMC with R^2 of 0.1 and rRMSE of 0.23 (see Fig. 6).

B. Differences in Plant Traits Between Vegetation Types

CHL, SPA, and PDMC varied widely among different vegetation types (see Fig. 8). Alpine meadow had higher values and spanned a broader range of canopy CHL and SPA than alpine and montane steppe (see Fig. 8). The alpine steppe had the highest

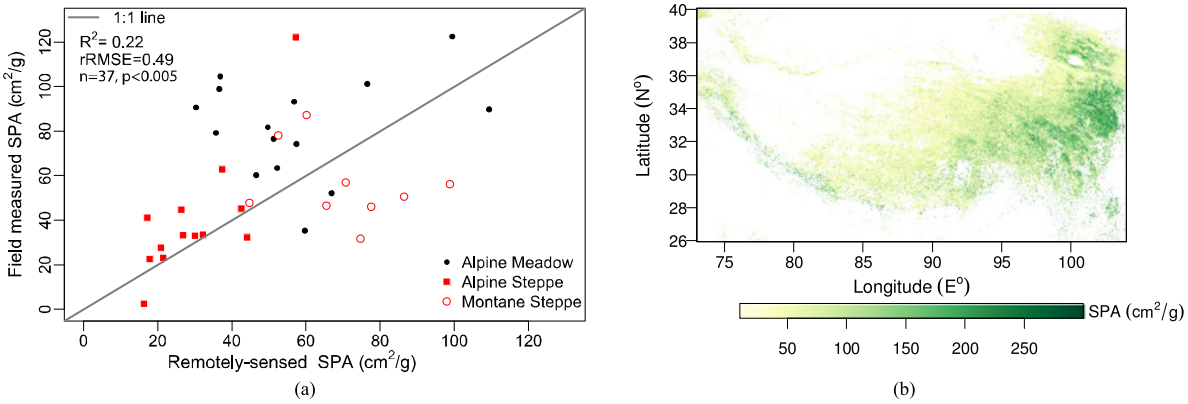

Fig. 5. Remotely sensed SPA on the Qinghai-Tibetan Plateau grasslands. (a) Scatter plot of field-measured SPA and remotely sensed SPA. (b) SPA with a spatial resolution of 500 m in the 2016 peak-growing season.

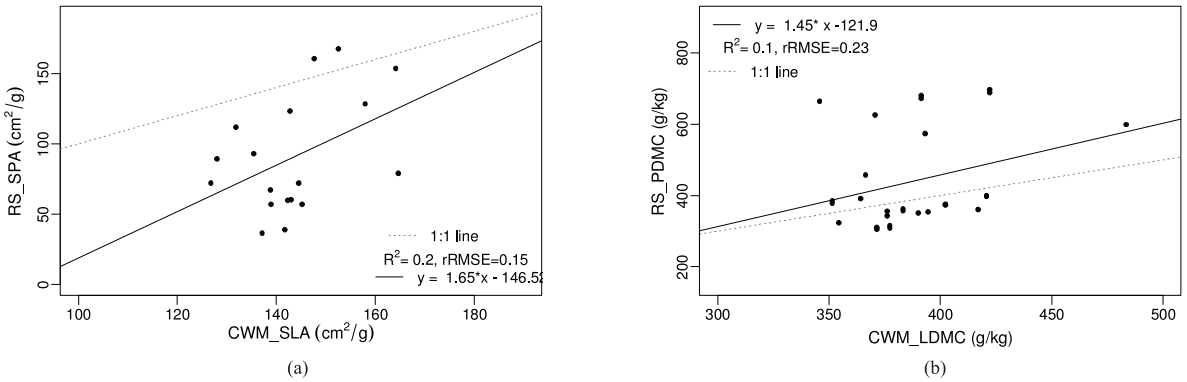

Fig. 6. Remotely sensed plant traits and literature-derived plant traits. (a) Relationship between remotely sensed SPA and literature-derived CWMs of SLA. (b) Relationship between remotely sensed PDMC and literature-derived CWMs of LDMC.

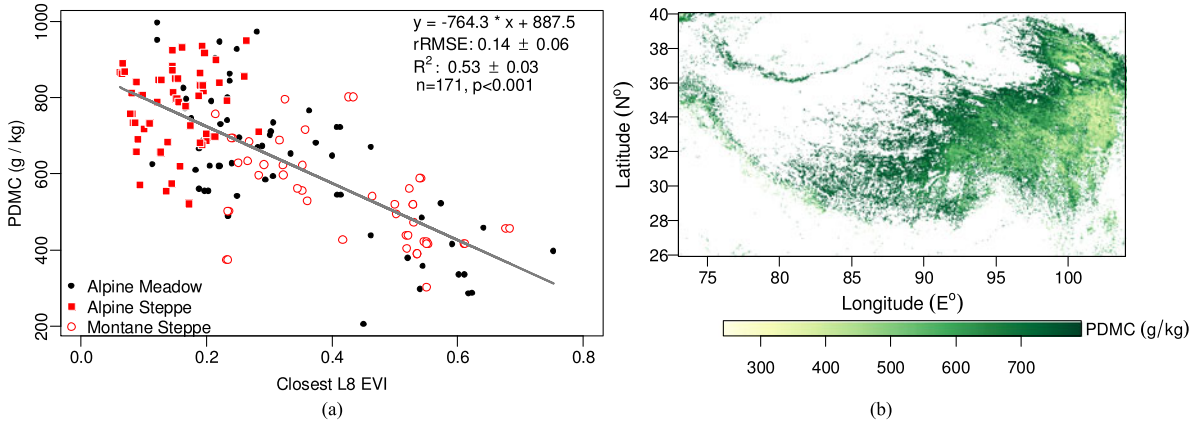

Fig. 7. Remotely sensed PDMC on the Qinghai-Tibetan Plateau grasslands. (a) Linear calibration model of EVI to predict PDMC. (b) PDMC with a spatial resolution of 30 m in the 2016 peak growing season.

PDMC but the lowest variability, whereas alpine meadow had the highest variability but lower PDMC (see Fig. 8). This pattern was consistent at both scales (1 m and 1 km).

V. Discussions

In this study, we found that plant traits of CHL, SPA, and PDMC can be retrieved over the complete Qinghai-Tibetan Plateau by statistical models developed from the field-measured plant traits and vegetation indices derived from the Landsat-8 and Sentinel-2 data. Below, we discuss:

1) the prediction accuracy of remotely sensed plant traits and their relation with the literature-derived CWMs of SLA and LDMC;
2) plant adaptation strategies of vegetation types as indicated by the observed trait differences;

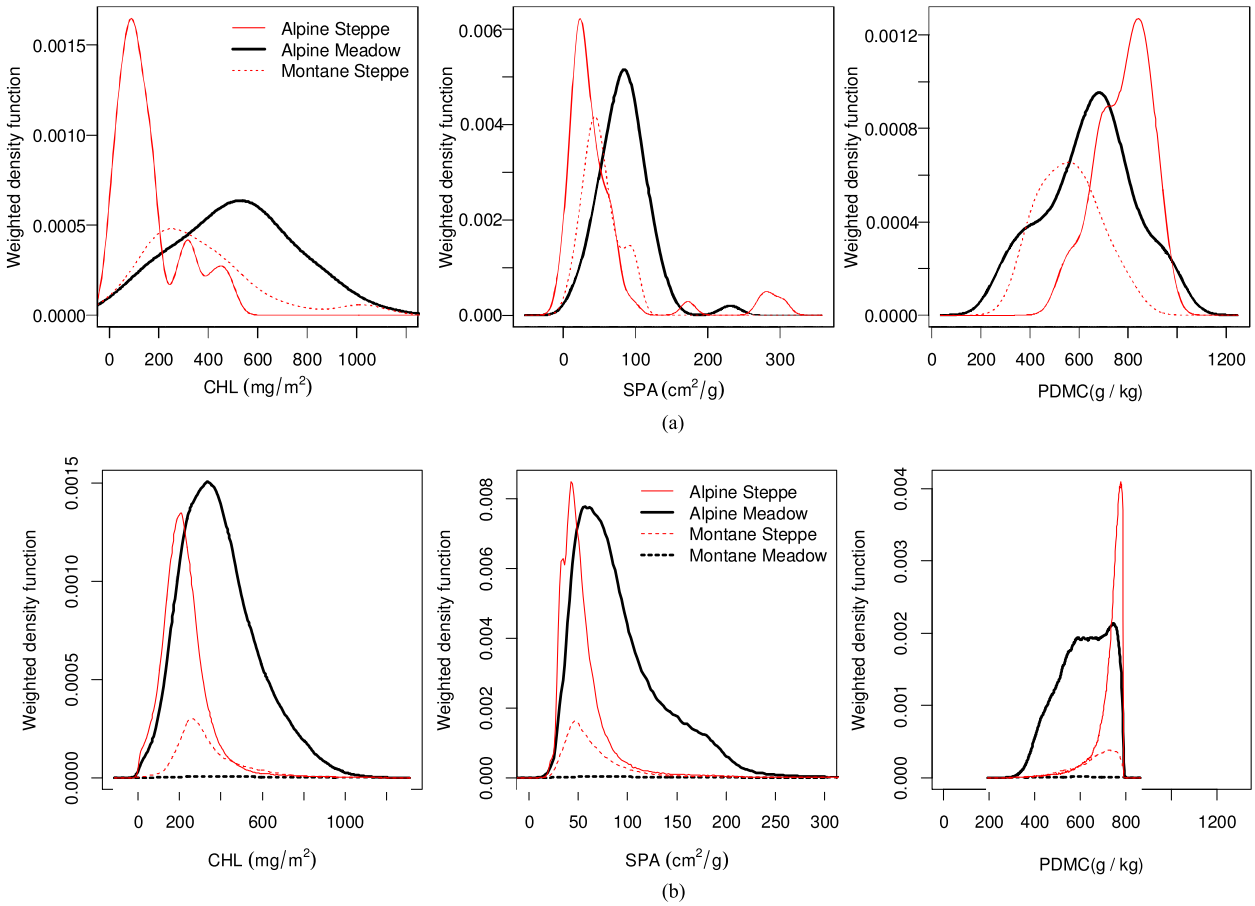

Fig. 8. Probability density functions of plant traits in different vegetation types. (a) One meter scale. (b) One kilometer scale.

3) potential implications of remotely sensed plant traits for ecosystem functioning in future studies.

A. Plant Traits

1) Canopy CHL: We tested the capability of Sentinel-2 red-edge vegetation indices to estimate canopy CHL on the Qinghai-Tibetan Plateau. We estimated canopy CHL through multiplying leaf CHL by PAI, a method often applied in croplands [55], [57]–[60]. The method is also applicable to diverse alpine grasslands on the Qinghai-Tibetan Plateau even though the prediction accuracy ($R^2 = 34\%$, rRMSE of 0.54) is lower than prediction accuracies typically reported for mono-species croplands [2], [19]. It is likely that the higher plant species diversity and corresponding higher spatial heterogeneity in PAI in natural grasslands are a main reason for this. Additionally, difficulties of measuring SPAD for small grass leaves may have affected the prediction accuracy.

We found that among the tested red-edge vegetation indices MCARI/ OSAVI was the best estimator of canopy CHL in alpine grasslands, presumably because it minimizes soil background effects and is resistant to PAI variation for low PAI values while still being sensitive to high CHL values [2]. TCARI/OSAVI had the lowest accuracy in predicting canopy CHL presumably because it was more affected by background information for PAI values < 0.5 [2]. A further explanation could be that TCARI/OSAVI was found to have a nonlinear relationship with PAI, changing from positive to negative at PAI $= 0.5$ [2]. This characteristic of TCARI/OSAVI might result in lower accuracy when applying a linear model for predicting canopy CHL.

2) Specific Plant Area (SPA): We found that remotely sensed SPA correlated to the field-measured values of SPA ($R^2 = 0.22$) and the literature-based CWMs of SLA ($R^2 = 0.2$). We found both field-measured and remotely sensed SPA were generally lower (-73 and -53 g/cm^2) than the reference CWMs of SLA. The reason for this underestimation was probably that SPA includes plant parts that have a lower surface to volume ratio than leaves. Even though remotely sensed SPA and literature-derived CWMs of SLA were obtained with vastly different methods we still found that they were correlated (see Fig. 6).

We showed that remotely sensed SPA at 500 m scale ranges from 10 to 231.2 cm^2/g over the entire Qinghai-Tibetan Plateau, leading to a wider range of values compared to existing studies [36], [66], [75]. This range is within the scope of CWMs of SLA values reported in the literature at a global scale. Kattge *et al.* [76] found that field-measured herb and grass CWMs of SLA ranged from 70 to 500 cm^2/g with an average of 200 cm^2/g in the northern hemisphere.

3) Plant Dry Matter Content (PDMC): Remotely sensed PDMC ($R^2 = 0.53$, rRMSE $= 13\%$) was estimated with higher

prediction accuracy than canopy CHL ($R^2 = 0.33$, rRMSE = 50%) and SPA ($R^2 = 0.22$, rRMSE = 49%). This study found that vegetation indices (e.g., EVI) correlated negatively with PDMC (see Fig. 7). The study area covers a large spatial gradient of precipitation (from more than 1000 to less than 100 mm/yr) [39], which influence leaf water content and biomass. Humid areas are characterized by higher leaf water content as well as biomass, leading to higher EVI compared with dry area. Therefore, EVI is positively correlated with leaf water content. The PDMC has an inverse relationship to leaf water content [26], thus EVI is negatively correlated with PDMC. This study found that differences in the visible and near-infrared regions of the spectra could explain variations of PDMC in alpine grasslands. Remotely sensed PDMC correlated with the literature-derived CWMs of LDMC on the Qinghai-Tibetan Plateau (see Fig. 6). However, the correlation was rather low and remotely sensed PDMC values were on average 54.7 g/kg higher than the literature-derived CWM of LDMC, presumably because non-leaf structures—which were considered as part of LDMC in this study—have lower water content than leaves.

B. Implication of Trait Variations Among Vegetation Types Under Global Change

Trait differences among vegetation types indicate different plant adaptation strategies [77]. Understanding these different plant strategies may help us to predict how ecosystems will respond to global change, especially for alpine plants on the Qinghai-Tibetan Plateau, which have adapted to low temperatures, and are expected to have developed unique survival strategies [31].

The trait differences between vegetation types indicate a tradeoff between plant productivity and persistence. We found a general East-to-West pattern of decreasing canopy CHL and SPA values and increasing PDMC values across the Qinghai-Tibetan Plateau. These spatial patterns of plant traits are related to the spatial distribution of vegetation types shifting from meadow to steppe along the East-West gradient, and further correspond to decreasing rainfall and increasing aridity toward the West [78]. Alpine meadows occur in environments beneficial to plant growth in terms of water availability and temperature [42], allowing plants to be fast in resource capturing and nutrient turnover [79], [80], leading to high photosynthetic rates and fast growth rates but low tissue density. This adaptation accounts for high CHL and SLA but low LDMC [81]–[83] of plants in alpine meadow and indicates a tradeoff between plant productivity and persistence [32], [84]. Alpine steppe grows in arid areas with low water availability and low soil fertility [42], where plants adapt to this resource-limited environment by decreasing leaf area in order to decrease evaporation, increase tissue density, and slow down photosynthesis and growth rate [81], [82]. This characteristic makes plants invest less in resource acquisition and more in structural tissue, which results in higher LDMC but lower SLA and canopy CHL content [81], [82]. In accordance with these hypotheses, we found that plants from alpine meadows had higher CHL and SPA but lower PDMC values than plants from alpine steppe for both field-measured and remotely sensed traits (see Fig. 8). Montane steppe and montane meadow grow at lower elevations and thus in warmer areas and are exposed to intermediate resource availability. These environmental conditions might explain why their trait values ranged between the values of alpine meadow and alpine steppe.

Potential changes of the vegetation-type distributions and plant traits on the Qinghai-Tibetan Plateau due to warming and increased precipitation [37], [85], [86] could be indicated by the natural spatial gradient of the vegetation-type distributions and plant traits toward the East. Because the warming and wetting trend on the Qinghai-Tibetan Plateau [83]–[85] are comparable to the spatial gradient of increasing temperature and water availability toward the East, this spatial pattern may enable a space-for-time approach to predict the potential changes of plant traits and vegetation types under global change. Because meadows occur in warmer and wetter environments, we speculate that the warming and increasing precipitation are more favorable for alpine meadows. Previous studies found that vegetation activity has increased in recent decades on the Qinghai-Tibetan Plateau because of the increased temperature [87], [88]. This trend of increased vegetation activity is more significant for alpine meadow than for the other vegetation types [89]. For the reasons stated above, we deduced that alpine meadows might benefit most on the Qinghai-Tibetan Plateau in a global-change setting. This suggests higher CHL and SLA but lower LDMC over the eastern part of the Qinghai-Tibetan Plateau in the future.

C. Potential Implication of Remotely Sensed Plant Traits on the Qinghai-Tibetan Plateau

We demonstrated that remotely sensed SPA and PDMC were related to CWMs of SLA and LDMC reported in earlier studies. Therefore, approximations between plant- and leaf-level traits may be a straightforward way to simplify trait measurement in alpine grasslands. Furthermore, maps of remotely sensed plant traits as presented in this study can lay the foundation for further ecological trait studies over large regions under global change.

Remotely sensed plant traits of CHL, SPA, and PDMC are predictors of ecosystem functioning and services on the Qinghai-Tibetan Plateau. CHL and SPA are closely related to plant nitrogen and define the photosynthetic capacity of vegetation [11], [25]; they therefore also affect the amount of carbon uptake of the ecosystem. Photosynthetic capacity and carbon uptake are especially important for the ecosystem on the Qinghai-Tibetan Plateau, where the photosynthetic rate is limited by low temperature, low air pressure, high wind speed, and high UV-B radiation [31]. LDMC has been shown to correlate negatively with potential relative growth rate and positively with leaf lifespan, which serves as an indicator of plant resistance to physical hazards and disturbance, plant digestibility, and rangeland quality [11]. Plants with higher LDMC tend to be physically tougher and thus are assumed to have higher resistance but lower plant digestibility.

Remotely sensed plant traits can hence facilitate future studies on how plants traits correlate to environmental variables and

land-use related variables such as grazing intensity. Traits and trait combinations vary with temperature, aridity, soil fertility, and grazing level [79], [90]. The prominent gradient in climate, soil properties, and grazing intensity on the Qinghai-Tibetan Plateau offers a convenient way to study how these different environmental factors correlate to plant traits. Previous studies for example suggested that SLA can express strong traits plasticity [91] and LDMC is sensitive to rainfall [92]. In another study, CHL was found to be positively correlated with grazing intensity up to medium grazing intensities because cattle excrement is the only external source of nutrients in these ecosystems [93] and increases nutrient availability for plants. These findings identified in local studies could be re-examined over larger spatial extent and in a spatially continuous way by making use of trait maps as presented in this study. This is particularly interesting as the environmental conditions and land-use management strategies vary widely over the Qinghai-Tibetan Plateau and it would hence be interesting to study how the relationships between plant traits and environmental and land-use variables depend on the location on the Plateau.

VI. Conclusion and Outlook

Based on statistical models between vegetation indices and field-measured plant traits, and by taking advantage of the Google Earth Engine cloud-computing platform, we derived the plant traits CHL, SPA, and PDMC across the entire Qinghai-Tibetan Plateau at the fine resolutions of 20, 500, and 30 m, respectively. Our results showed that the plant traits of CHL, SPA, and PDMC could be predicted using satellite data of Sentinel-2 (20 m) and Landsat-8 (30 m) as well as the MODIS LAI product (500 m), with R^2 of 0.34, 0.22, and 0.53, respectively.

We found that the canopy CHL and SPA values of alpine meadows were higher and had a wider range than the values observed for the alpine steppe. On the contrary, PDMC values were lower and more narrowly distributed in alpine meadow than in alpine steppe. These plant trait differences among vegetation types indicate tradeoffs between plant productivity and persistence, describing different plant strategies.

We demonstrated that remotely sensed and field-measured SPA and PDMC correlated with the literature-derived CWMs of SLA and LDMC even though the correlations were not very strong most likely because the datasets were measured at different times and spatial scales. It is conceivable that the correlations could be improved if measurements were conducted at the same time and spatial scale. More research is needed to further test the hypothesis that leaf-level trait measurement of CWMs of SLA and LDMC are comparable to field-measured and remotely sensed SPA and PDMC in grassland. Strengthening the hypothesis would be beneficial for simplifying the study of plant traits and also facilitate trait estimation using remote-sensing technologies. The latter would also enable repeated trait assessments via remote sensing, which would enable the monitoring of plant traits. This could be key for a timely identification of potential ecosystem degradations on the Qinghai-Tibetan Plateau.

Acknowledgment

The authors would like to thank G. Du (Lanzhou University), W. Qi (Lanzhou University), K. Niu (Nanjing University), and W. Wang (Qinghai Normal University) for their help and support with field-data collection; D. Fawcett, F. Schneider, and D. Braun for their language corrections and helpful comments; and anonymous reviewers who provided useful comments to the manuscript. We are grateful to the support of the University of Zurich Research Priority Program on 'Global Change and Biodiversity' (URPP GCB).

References

[1] C. Violle *et al.*, "Let the concept of trait be functional!," *Oikos*, vol. 116, no. 5, pp. 882–892, 2007.
[2] C. Wu, Z. Niu, Q. Tang, and W. Huang, "Estimating chlorophyll content from hyperspectral vegetation indices: Modeling and validation," *Agricultural Forest Meteorol.*, vol. 148, nos. 8–9, pp. 1230–1241, 2008.
[3] A. A. Gitelson, Y. Peng, T. J. Arkebauer, and J. Schepers, "Relationships between gross primary production, green LAI, and canopy chlorophyll content in maize: Implications for remote sensing of primary production," *Remote Sens. Environ.*, vol. 144, pp. 65–72, Mar. 2014.
[4] E. J. Forrestel, M. J. Donoghue, E. J. Edwards, W. Jetz, J. C. O. du Toit, and M. D. Smith, "Different clades and traits yield similar grassland functional responses," *Proc. Nat. Acad. Sci.*, vol. 114, no. 4, pp. 705–710, 2017.
[5] N. Pettorelli *et al.*, "Framing the concept of satellite remote sensing essential biodiversity variables: Challenges and future directions," *Remote Sens. Ecol. Conservation*, vol. 2, no. 3, pp. 122–131, 2016.
[6] A. K. Skidmore *et al.*, "Environmental science: Agree on biodiversity metrics to track from space," *Nature*, vol. 523, no. 7561, pp. 403–405, 2015.
[7] B. Sakschewski *et al.*, "Leaf and stem economics spectra drive diversity of functional plant traits in a dynamic global vegetation model," *Global Change Biol.*, vol. 21, no. 7, pp. 2711–2725, Jan. 2015.
[8] C. Pappas, S. Fatichi, and P. Burlando, "Modeling terrestrial carbon and water dynamics across climatic gradients: Does plant trait diversity matter?" *New Phytologist*, vol. 209, no. 1, pp. 137–151, 2016.
[9] G. Miehe, S. Miehe, K. Kaiser, J. Liu, and X. Zhao, "Status and dynamics of the Kobresia pygmaea ecosystem on the Tibetan plateau," *Ambio*, vol. 37, no. 4, pp. 272–279, 2008.
[10] G. Miehe *et al.*, "Alpine steppe plant communities of the Tibetan highlands," *Appl. Vegetation Sci.*, vol. 14, no. 4, pp. 547–560, 2011.
[11] N. Pérez-Harguindeguy *et al.*, "New handbook for standardized measurement of plant functional traits worldwide," *Aust. J. Botany*, vol. 61, no. 34, pp. 167–234, 2013.
[12] H. Feilhauer, B. Somers, and S. van der Linden, "Optical trait indicators for remote sensing of plant species composition: Predictive power and seasonal variability," *Ecological Indicators*, vol. 73, pp. 825–833, 2017.
[13] L. Homolová, Z. Malenovský, J. G. P. W. Clevers, G. García-Santos, and M. E. Schaepman, "Review of optical-based remote sensing for plant trait mapping," *Ecological Complexity*, vol. 15, pp. 1–16, 2013.
[14] J.-B. Féret *et al.*, "Optimizing spectral indices and chemometric analysis of leaf chemical properties using radiative transfer modeling," *Remote Sens. Environ.*, vol. 115, no. 10, pp. 2742–2750, 2011.
[15] G. le Maire *et al.*, "Calibration and validation of hyperspectral indices for the estimation of broadleaved forest leaf chlorophyll content, leaf mass per area, leaf area index and leaf canopy biomass," *Remote Sens. Environ.*, vol. 112, no. 10, pp. 3846–3864, Oct. 2008.
[16] A. M. Ali, R. Darvishzadeh, A. K. Skidmore, I. van Duren, U. Heiden, and M. Heurich, "Estimating leaf functional traits by inversion of PROSPECT: Assessing leaf dry matter content and specific leaf area in mixed mountainous forest," *Int. J. Appl. Earth Observ. Geoinf.*, vol. 45, pp. 66–76, 2016.
[17] S. Jacquemoud *et al.*, "PROSPECT + SAIL models: A review of use for vegetation characterization," *Remote Sens. Environ.*, vol. 113, no. suppl. 1, pp. S56–S66, 2009.
[18] M. Vincini, S. Amaducci, and E. Frazzi, "Empirical estimation of leaf chlorophyll density in winter wheat canopies using Sentinel-2 spectral resolution," *IEEE Trans. Geosci. Remote Sens.*, vol. 52, no. 6, pp. 3220–3235, Jun. 2014.

[19] M. Schlemmera *et al.*, "Remote estimation of nitrogen and chlorophyll contents in maize at leaf and canopy levels," *Int. J. Appl. Earth Observ. Geoinf.*, vol. 25, no. 1, pp. 47–54, 2013.

[20] S. L. Ustin *et al.*, "Retrieval of foliar information about plant pigment systems from high resolution spectroscopy," *Remote Sens. Environ.*, vol. 113, no. suppl. 1, pp. S67–S77, 2009.

[21] A. M. Ali, R. Darvishzadeh, A. K. Skidmore, and I. van Duren, "Specific leaf area estimation from leaf and canopy reflectance through optimization and validation of vegetation indices," *Agricultural Forest Meteorol.*, vol. 236, pp. 162–174, 2017.

[22] A. M. Ali, R. Darvishzadeh, and A. K. Skidmore, "Retrieval of specific leaf area from landsat-8 surface reflectance data using statistical and physical models," *IEEE J. Sel. Topics Appl. Earth Observ. Remote Sens.*, vol. 10, no. 6, pp. 3529–3536, Aug. 2017.

[23] G. P. Asner and R. E. Martin, "Spectral and chemical analysis of tropical forests: Scaling from leaf to canopy levels," *Remote Sens. Environ.*, vol. 112, no. 10, pp. 3958–3970, 2008.

[24] G. P. Asner *et al.*, "Taxonomy and remote sensing of leaf mass per area (LMA) in humid tropical forests," *Ecological Appl.*, vol. 21, no. 1, pp. 85–98, 2011.

[25] A. M. Ali, R. Darvishzadeh, A. K. Skidmore, and I. Van Duren, "Effects of canopy structural variables on retrieval of leaf dry matter content and specific leaf area from remotely sensed data," *IEEE J. Sel. Topics Appl. Earth Observ. Remote Sens.*, vol. 9, no. 2, pp. 898–909, Feb. 2016.

[26] H. D. Roelofsen, P. M. van Bodegom, L. Kooistra, and J. P. M. Witte, "Predicting leaf traits of herbaceous species from their spectral characteristics," *Ecol. Evol.*, vol. 4, no. 6, pp. 706–719, 2014.

[27] A. Capolupo, L. Kooistra, C. Berendonk, L. Boccia, and J. Suomalainen, "Estimating plant traits of grasslands from UAV-acquired hyperspectral images: A comparison of statistical approaches," *ISPRS Int. J. Geo-Inf.*, vol. 4, no. 4, pp. 2792–2820, 2015.

[28] H. D. Roelofsen, P. M. van Bodegom, L. Kooistra, and J. P. M. Witte, "Trait estimation in herbaceous plant assemblages from in situ canopy spectra," *Remote Sens*., vol. 5, no. 12, pp. 6323–6345, 2013.

[29] M. Vohland and T. Jarmer, "Estimating structural and biochemical parameters for grassland from spectroradiometer data by radiative transfer modelling (PROSPECT+SAIL)," *Int. J. Remote Sens.*, vol. 29, no. 1, pp. 191–209, 2008.

[30] S. Punalekar *et al.*, "Characterization of a highly biodiverse floodplain meadow using hyperspectral remote sensing within a plant functional trait framework," *Remote Sens*., vol. 8, no. 2, 2016, Art. no. 112.

[31] J. S. He *et al.*, "A test of the generality of leaf trait relationships on the Tibetan plateau," *New Phytologist*, vol. 170, no. 4, pp. 835–848, 2006.

[32] J. S. He, X. Wang, D. F. B. Flynn, L. Wang, B. Schmid, and J. Fang, "Taxonomic, phylogenetic, and environmental trade-offs between leaf productivity and persistence," *Ecology*, vol. 90, no. 10, pp. 2779–2791, 2009.

[33] K. Niu, J. Messier, J.-S. He, and M. J. Lechowicz, "The effects of grazing on foliar trait diversity and niche differentiation in Tibetan alpine meadows," *Ecosphere*, vol. 6, pp. 1–15, Sep. 2015.

[34] Z. H. Zhu, X. A. Wang, Y. N. Li, G. Wang, and H. Guo, "Predicting plant traits and functional types response to grazing in an alpine shrub meadow on the Qinghai-Tibet Plateau," *Sci. China Earth Sci.*, vol. 55, no. 5, pp. 837–851, 2012.

[35] J. Sun, X. Wang, G. Cheng, J. Wu, J. Hong, and S. Niu, "Effects of grazing regimes on plant traits and soil nutrients in an alpine steppe, northern Tibetan plateau," *PLoS One*, vol. 9, no. 9, 2014, Art. no. e108821.

[36] W. L. Ma *et al.*, "Changes in individual plant traits and biomass allocation in alpine meadow with elevation variation on the Qinghai-Tibetan plateau," *Sci. China Life Sci.*, vol. 53, no. 9, pp. 1142–1151, 2010.

[37] T. Yao *et al.*, "Third pole environment (TPE)," *Environ. Develop.*, vol. 3, no. 1, pp. 52–64, 2012.

[38] R. B. Harris, "Rangeland degradation on the Qinghai-Tibetan plateau: A review of the evidence of its magnitude and causes," *J. Arid Environ.*, vol. 74, no. 1, pp. 1–12, 2010.

[39] X. Chen, S. An, D. W. Inouye, and M. D. Schwartz, "Temperature and snowfall trigger alpine vegetation green-up on the world's roof," *Global Change Biol.*, vol. 21, no. 10, pp. 3635–3646, 2015.

[40] X. Hou, *Vegetation Altas of China*. Beijing, China: Science, 2001.

[41] X. Li *et al.*, "Comparative proteomics analyses of Kobresia pygmaea adaptation to environment along an elevational gradient on the central Tibetan Plateau," *PLoS One*, vol. 9, no. 6, 2014, Art. no. e98410.

[42] G. Miehe *et al.*, "Resilience or vulnerability? Vegetation patterns of a Central Tibetan pastoral ecotone," in Steppe ecossystems: Biological diversity, management and restoration. Nova Science Publishers, Incorporated, 2013, pp. 111–151.

[43] J. Ni and U. Herzschuh, "Simulating biome distribution on the Tibetan plateau using a modified global vegetation model," *Arctic, Antarctic Alpine Res.*, vol. 43, no. 3, pp. 429–441, 2011.

[44] N. Gorelick, M. Hancher, M. Dixon, S. Ilyushchenko, D. Thau, and R. Moore, "Google earth engine: Planetary-scale geospatial analysis for everyone," *Remote Sens. Environ.*, vol. 202, pp. 18–27, 2017.

[45] D. P. Roy *et al.*, "Landsat-8: Science and product vision for terrestrial global change research," *Remote Sens. Environ.*, vol. 145, pp. 154–172, 2014.

[46] M. Drusch *et al.*, "Sentinel-2: ESA's optical high-resolution mission for GMES operational services," *Remote Sens. Environ.*, vol. 120, pp. 25–36, 2012.

[47] M. A. Friedl *et al.*, "MODIS Collection 5 global land cover: Algorithm refinements and characterization of new datasets," *Remote Sens. Environ.*, vol. 114, no. 1, pp. 168–182, 2010.

[48] R. Myneni, Y. Knyazikhin, and T. Park, "MCD15A2H MODIS/terra+aqua leaf area index/FPAR 8?day L4 global 500 m SIN grid V006," *NASA EOSDIS Land Process. DAAC, Dataset*, 2015.

[49] S. Foga *et al.*, "Cloud detection algorithm comparison and validation for operational landsat data products," *Remote Sens. Environ.*, vol. 194, pp. 379–390, 2017.

[50] Z. Zhu and C. E. Woodcock, "Object-based cloud and cloud shadow detection in Landsat imagery," *Remote Sens. Environ.*, vol. 118, pp. 83–94, 2012.

[51] W. Yang *et al.*, "Analysis of leaf area index and fraction of PAR absorbed by vegetation products from the terra MODIS sensor: 2000-2005," *IEEE Trans. Geosci. Remote Sens.*, vol. 44, no. 7, pp. 1829–1841, Jul. 2006.

[52] K. Yan *et al.*, "Evaluation of MODIS LAI/FPAR product collection 6. Part 2: Validation and intercomparison," *Remote Sens*., vol. 8, no. 6, 2016, Art. no. 359.

[53] R. R. Irish, J. L. Barker, S. N. Goward, and T. Arvidson, "Characterization of the landsat-7 ETM+ automated cloud-cover assessment (ACCA) algorithm," *Photogramm. Eng. Remote Sens.*, vol. 72, no. 10, pp. 1179–1188, 2006.

[54] L. W. Lehnert *et al.*, "Retrieval of grassland plant coverage on the Tibetan plateau based on a multi-scale, multi-sensor and multi-method approach," *Remote Sens. Environ.*, vol. 164, pp. 197–207, 2015.

[55] R. Darvishzadeh, A. Skidmore, M. Schlerf, and C. Atzberger, "Inversion of a radiative transfer model for estimating vegetation LAI and chlorophyll in a heterogeneous grassland," *Remote Sens. Environ.*, vol. 112, no. 5, pp. 2592–2604, May 2008.

[56] S. Ghosh, D. R. Mishra, and A. A. Gitelson, "Long-term monitoring of biophysical characteristics of tidal wetlands in the northern gulf of Mexico - A methodological approach using MODIS," *Remote Sens. Environ.*, vol. 173, pp. 39–58, 2016.

[57] A. A. Gitelson, A. Viña, V. Ciganda, D. C. Rundquist, and T. J. Arkebauer, "Remote estimation of canopy chlorophyll content in crops," *Geophys. Res. Lett.*, vol. 32, no. 8, pp. 1–4, 2005.

[58] C. Wu, Z. Niu, and S. Gao, "The potential of the satellite derived green chlorophyll index for estimating midday light use efficiency in maize, coniferous forest and grassland," *Ecological Indicators*, vol. 14, no. 1, pp. 66–73, 2012.

[59] Y. Peng and A. A. Gitelson, "Application of chlorophyll-related vegetation indices for remote estimation of maize productivity," *Agricultural Forest Meteorol.*, vol. 151, no. 9, pp. 1267–1276, 2011.

[60] R. Darvishzadeh, A. Skidmore, M. Schlerf, C. Atzberger, F. Corsi, and M. Cho, "LAI and chlorophyll estimation for a heterogeneous grassland using hyperspectral measurements," *ISPRS J. Photogramm. Remote Sens.*, vol. 63, no. 4, pp. 409–426, Jul. 2008.

[61] E. Mougin, V. Demarez, M. Diawara, P. Hiernaux, N. Soumaguel, and A. Berg, "Estimation of LAI, fAPAR and fCover of sahel rangelands (Gourma, Mali)," *Agricultural Forest Meteorol.*, vol. 198, pp. 155–167, 2014.

[62] W. B. Sea, P. Choler, J. Beringer, R. A. Weinmann, L. B. Hutley, and R. Leuning, "Documenting improvement in leaf area index estimates from MODIS using hemispherical photos for Australian savannas," *Agricultural Forest Meteorol.*, vol. 151, no. 11, pp. 1453–1461, 2011.

[63] S. Lavorel *et al.*, "Assessing functional diversity in the field - methodology matters!," *Funct. Ecol.*, vol. 22, no. 1, pp. 134–147, 2008.

[64] F. D. Schneider *et al.*, "Mapping functional diversity from remotely sensed morphological and physiological forest traits," *Nature Commun.*, vol. 8, no. 1, 2017, Art. no. 1441.
[65] J. S. He *et al.*, "A test of the generality of leaf trait relationships on the Tibetan plateau," *New Phytologist*, vol. 170, no. 4, pp. 835–848, 2006.
[66] L. Chen *et al.*, "UV radiation is the primary factor driving the variation in leaf phenolics across Chinese grasslands," *Ecol. Evol.*, vol. 3, no. 14, pp. 4696–4710, 2013.
[67] X. Zhou, Y. Wang, P. Zhang, Z. Guo, C. Chu, and G. Du, "The effects of fertilization on the trait-abundance relationships in a Tibetan alpine meadow community," *J. Plant Ecol.*, vol. 9, no. 2, pp. 144–152, 2016.
[68] K. Niu, J. S. He, S. Zhang, and M. J. Lechowicz, "Tradeoffs between forage quality and soil fertility: Lessons from Himalayan rangelands," *Agriculture, Ecosyst. Environ.*, vol. 234, pp. 31–39, 2016.
[69] A. A. Gitelson, Y. Peng, and K. F. Huemmrich, "Relationship between fraction of radiation absorbed by photosynthesizing maize and soybean canopies and NDVI from remotely sensed data taken at close range and from MODIS 250m resolution data," *Remote Sens. Environ.*, vol. 147, pp. 108–120, 2014.
[70] A. Ramoelo, A. K. Skidmore, M. Schlerf, I. M. A. Heitkönig, R. Mathieu, and M. A. Cho, "Savanna grass nitrogen to phosphorous ratio estimation using field spectroscopy and the potential for estimation with imaging spectroscopy," *Int. J. Appl. Earth Observ. Geoinf.*, vol. 23, no. 1, pp. 334–343, 2013.
[71] P. J. Zarco-Tejada, J. R. Miller, T. L. Noland, G. H. Mohammed, and P. H. Sampson, "Scaling-up and model inversion methods with narrow-band optical indices for chlorophyll content estimation in closed forest canopies with hyperspectral data," *IEEE Trans. Geosci. Remote Sens.*, vol. 39, no. 7, pp. 1491–1507, Jul. 2001.
[72] J. G. P. W. Clevers and L. Kooistra, "Using hyperspectral remote sensing data for retrieving canopy chlorophyll and nitrogen content," *IEEE J. Sel. Topics Appl. Earth Observ. Remote Sens.*, vol. 5, no. 2, pp. 574–583, Apr. 2012.
[73] S. Díaz *et al.*, "The global spectrum of plant form and function," *Nature*, vol. 529, no. 7585, pp. 167–171, 2015.
[74] T. Duong, "Ks: Kernel density estimation and kernel discriminant analysis for multivariate data in R," *J. Statist. Softw.*, vol. 21, no. 7, pp. 1–16, 2007.
[75] W. Li *et al.*, "Community-weighted mean traits but not functional diversity determine the changes in soil properties during wetland drying on the Tibetan plateau," *Solid Earth*, vol. 8, no. 1, pp. 137–147, 2017.
[76] J. Kattge *et al.*, "TRY - A global database of plant traits," *Global Change Biol.*, vol. 17, no. 9, pp. 2905–2935, 2011.
[77] T. Kattenborn, F. E. Fassnacht, S. Pierce, J. Lopatin, J. P. Grime, and S. Schmidtlein, "Linking plant strategies and plant traits derived by radiative transfer modelling," *J. Vegetation Sci.*, vol. 28, no. 4, pp. 717–727, 2017.
[78] G. Miehe *et al.*, "Plant communities of central Tibetan pastures in the Alpine Steppe/Kobresia pygmaea ecotone," *J. Arid Environ.*, vol. 75, no. 8, pp. 711–723, 2011.
[79] J. S. He *et al.*, "Taxonomic identity, phylogeny, climate and soil fertility as drivers of leaf traits across Chinese grassland biomes," *J. Plant Res.*, vol. 123, no. 4, pp. 551–561, 2010.
[80] F. S. Chapin, "The mineral nutrition of wild plants," *Annu. Rev.*, vol. 11, no. 1980, pp. 233–260, 1980.
[81] A. K. Schweiger, M. Schütz, A. C. Risch, M. Kneubühler, R. Haller, and M. E. Schaepman, "How to predict plant functional types using imaging spectroscopy: Linking vegetation community traits, plant functional types and spectral response," *Methods Ecol. Evol.*, vol. 8, no. 1, pp. 86–95, 2017.
[82] S. Pierce *et al.*, "A global method for calculating plant CSR ecological strategies applied across biomes world-wide," *Funct. Ecol.*, vol. 31, no. 2, pp. 444–457, 2017.
[83] S. Díaz *et al.*, "The plant traits that drive ecosystems: Evidence from three continents," *J. Vegetation Sci.*, vol. 15, no. 3, pp. 295–304, 2004.
[84] M. Diemer, "Leaf lifespans of high-elevation, aseasonal Andean shrub species in relation to leaf traits and leaf habit," *Global Ecol. Biogeography*, vol. 7, no. 6, pp. 457–465, 1998.
[85] S. Kang, Y. Xu, Q. You, W.-A. Flügel, N. Pepin, and T. Yao, "Review of climate and cryospheric change in the Tibetan Plateau," *Environ. Res. Lett.*, vol. 5, no. 1, 2010, Art. no. 15101.
[86] Q. You, K. Fraedrich, G. Ren, N. Pepin, and S. Kang, "Variability of temperature in the Tibetan Plateau based on homogenized surface stations and reanalysis data," *Int. J. Climatol.*, vol. 33, no. 6, pp. 1337–1347, 2013.
[87] S. Piao, J. Fang, and H. E. Jinsheng, "Variations in vegetation net primary production in the Qinghai-Xizang Plateau, China, from 1982 to 1999," *Clim. Change*, vol. 74, no. 1–3, pp. 253–267, 2006.
[88] J. Peng, Z. Liu, Y. Liu, J. Wu, and Y. Han, "Trend analysis of vegetation dynamics in Qinghai-Tibet plateau using hurst exponent," *Ecological Indicators*, vol. 14, no. 1, pp. 28–39, 2012.
[89] G. Zhang, Y. Zhang, J. Dong, and X. Xiao, "Green-up dates in the Tibetan Plateau have continuously advanced from 1982 to 2011," *Proc. Nat. Acad. Sci.*, vol. 110, no. 11, pp. 4309–4314, 2013.
[90] K. Niu, S. Zhang, B. Zhao, and G. Du, "Linking grazing response of species abundance to functional traits in the Tibetan alpine meadow," *Plant Soil*, vol. 330, no. 1, pp. 215–223, 2010.
[91] B. Shipley, F. De Bello, J. H. C. Cornelissen, E. Laliberté, D. C. Laughlin, and P. B. Reich, "Reinforcing loose foundation stones in trait-based plant ecology," *Oecologia*, vol. 180, no. 4, pp. 923–931, 2016.
[92] R. J. Pakeman, "Leaf dry matter content predicts herbivore productivity, but its functional diversity is positively related to resilience in grasslands," *PLoS One*, vol. 9, no. 7, pp. 1–6, 2014.
[93] L. W. Lehnert, H. Meyer, N. Meyer, C. Reudenbach, and J. Bendix, "A hyperspectral indicator system for rangeland degradation on the Tibetan Plateau: A case study towards spaceborne monitoring," *Ecological Indicators*, vol. 39, pp. 54–64, 2014.
[94] T. Farr *et al.*, "The shuttle radar topography mission," *Rev. Geophys.*, vol. 45, no. 2005, pp. 1–33, 2007.
[95] A. A. Gitelson, Y. Gritz †, and M. N. Merzlyak, "Relationships between leaf chlorophyll content and spectral reflectance and algorithms for non-destructive chlorophyll assessment in higher plant leaves," *J. Plant Physiol.*, vol. 160, no. 3, pp. 271–282, 2003.
[96] A. A. Gitelson, G. P. Keydan, and M. N. Merzlyak, "Three-band model for noninvasive estimation of chlorophyll, carotenoids, and anthocyanin contents in higher plant leaves," *Geophys. Res. Lett.*, vol. 33, no. 11, pp. 2–6, 2006.
[97] D. Haboudane, N. Tremblay, J. R. Miller, and P. Vigneault, "Remote estimation of crop chlorophyll content using spectral indices derived from hyperspectral data," *IEEE Trans. Geosci. Remote Sens.*, vol. 46, no. 2, pp. 423–436, Feb. 2008.
[98] D. Haboudane, J. R. Miller, N. Tremblay, P. J. Zarco-Tejada, and L. Dextraze, "Integrated narrow-band vegetation indices for prediction of crop chlorophyll content for application to precision agriculture," *Remote Sens. Environ.*, vol. 81, nos. 2–3, pp. 416–426, Aug. 2002.
[99] A. R. Huete, H. Q. Liu, K. Batchily, and W. Van Leeuwen, "A comparison of vegetation indices over a global set of TM images for EOS-MODIS," *Remote Sens. Environ.*, vol. 59, no. 3, pp. 440–451, Mar. 1997.
[100] A. R. Huete and R. D. Jackson, "Soil and atmosphere influences on the spectra of partial canopies," *Remote Sens. Environ.*, vol. 25, no. 1, pp. 89–105, Jun. 1988.
[101] C. J. Tucker, "Red and photographic infrared linear combinations for monitoring vegetation," *Remote Sens. Environ.*, vol. 8, no. 2, pp. 127–150, May 1979.
[102] J. Qi, A. Chehbouni, A. R. Huete, Y. H. Kerr, and S. Sorooshian, "A modified soil adjusted vegetation index," *Remote Sens. Environ.*, vol. 48, no. 2, pp. 119–126, 1994.

Chengxiu Li received the B.A.Sc. degree in resources science and engineering from Beijing Normal University, Beijing, China, in 2010. She received the M.Sc. degree in geography from Lanzhou University, Lanzhou, China, in 2014. Her master study focused on "monitoring glacier and snow cover change in Western Kunlun Mountains." She is currently pursuing the Ph.D. degree in grassland ecology at the Remote Sensing Laboratories, University of Zürich, Zürich, Switzerland.

From 2010 to 2011, she was a Geography Teacher with the Affiliated Middle School, Inner Mongolia Normal University, China. In 2014, she joined the Remote Sensing Laboratories, Department of Geography, University of Zurich. Her research interests include mapping plant traits, and understanding how environmental variables and human activities influence and alter plant traits.

Hendrik Wulf received the Ph.D. degree in earth and environmental science from the University of Potsdam, Potsdam, Germany, in 2011, with the thesis on "Seasonal precipitation, river discharge, and sediment flux in the western Himalaya."

From 2012 to 2013, he was a Postdoctoral Researcher wih the Remote Sensing Unit, GFZ German Research Centre for Geosciences, working on the Science Plan of the EnMAP (Environmental Mapping and Analysis Program) satellite mission. From 2013 onwards, he is a Research Associate with the Remote Sensing Laboratories, University of Zurich, Zurich, Switzerland.

Bernhard Schmid received the Ph.D. degree in biology from the University of Zürich, Zürich, Switzerland, in 1980.

After postdoctoral stays in North Wales and with Harvard University, he was a Professor of conservation biology with the University of Basel before becoming a Professor of environmental sciences and the founding director of the corresponding Institute with the University of Zürich, Zurich, Switzerland. He is involved in several large-scale biodiversity experiments. His main research interests include experimental plant ecology and biodiversity–ecosystem functioning relationships.

Jin-Sheng He received the M.Sc. and Ph.D. degrees in ecology from the Chinese Academy of Sciences (Institute of Botany), Beijing, China, in 1991 and 1998, respectively.

From 1992-2002, he was a Postdoctoral Researcher with the Organismic and Evolutionary Biology, Harvard University, Cambridge, MA, USA. In 2002, he joined the Department of Ecology, College of Urban and Environmental Sciences, Peking University. From 2009 to 2016, he was an Adjunct Professor with the Northwest Institute of Plateau Biology, Chinese Academy of Sciences. He is currently the Director with the State Key Laboratory of Grassland and Agro-ecosystems, Lanzhou University, Lanzhou, China. His lab focuses on how global changes affect terrestrial ecosystems, in particular the alpine grassland on the Tibetan Plateau. Recently, his lab has focused on three general areas: 1) Understanding how climate change alters above- and below-ground biodiversity and ecosystem functioning; 2) Understanding connections among soil organisms, herbivores, plants, and ecosystem function; and 3) Understanding the scale-dependent interactions of shifting ecosystem composition, phenology, and ecological processes.

Michael E. Schaepman (M'05–SM'07) received M.Sc. and Ph.D. degrees in geography from the University of Zurich (UZH), Zurich, Switzerland, in 1993 and 1998, respectively.

In 1999, he was Postdoctoral Researcher with the Optical Sciences Center, University of Arizona, Tucson, AZ, USA. In 2000, he was Project Manager of the APEX imaging spectrometer jointly with the European Space Agency. In 2003, he became a Full Chair with the Geoinformation Science and Remote Sensing Laboratory, Wageningen University, Wageningen, The Netherlands. Since 2009, he has been a Full Chair of remote sensing with UZH, where he is currently heading the Remote Sensing Laboratories, Department of Geography. He is currently the Codirector of the University Research Priority Program on "Global Change and Biodiversity" and Vice President of Veterinary Medicine and Natural Sciences. His research interests include computational earth sciences using remote sensing and physical models, with a particular focus on the land–atmosphere interface using imaging spectroscopy.